EARTHQUAKE ENGINEERING AND STRUCTURAL DYNAMICS, VOL. 26, 571–591 (1997)

RIGIDITY–PLASTICITY–VISCOSITY: CAN ELECTRORHEOLOGICAL DAMPERS PROTECT BASE-ISOLATED STRUCTURES FROM NEAR-SOURCE GROUND MOTIONS?

NICOS MAKRIS*

Department of Civil and Environmental Engineering, SEMM, University of California at Berkeley, MC 1710, Berkeley, CA 94720, U.S.A.

SUMMARY

The concept of seismic protection by lengthening the fundamental period of the structure has been implemented through a number of isolation systems. While flexible isolation systems can effectively protect structures from earthquakes containing high frequencies and sharp accelerations, they might amplify the response of the structure when subjected to rapid, long-period motions. In this case of long period excitations the stiff superstructure should be 'locked' to the ground, rather than be supported on flexible bearings. This paper shows through a comprehensive analytical study that a practical solution to this problem is to provide additional rigidity to the structure using a friction-type mechanism (rigid-plastic behaviour). The presence of friction-type forces reduce substantially the relative displacements of a single-degree-of-freedom structure by keeping accelerations at low levels; however, they are responsible for the presence of permanent displacements. Accordingly, the use of controllable fluid dampers is proposed and it is shown that they can be a practical solution to the problem. The response of a single-degree-of-freedom base-isolated structures is investigated, and the feasibility of a proposed electrorheological damper to deliver the required forces is discussed. © 1997 by John Wiley & Sons, Ltd.

KEY WORDS: controllable fluid dampers; seismic isolated structures; near-source ground motions

INTRODUCTION

During the last two decades considerable advances have been accomplished in the area of seismic protection of structures due to developments in base isolation and supplemental energy dissipation. New promising systems have been developed which can be incorporated in structures to improve their response when excited by earthquakes.[1] These systems also known as earthquake-protective systems consist of passive, semiactive or active devices and can considerably minimize the seismic demand of buildings and bridges. In this paper it is shown that electrorheological dampers or other controllable fluid dampers can be a practical solution to the challenging problem of protecting flexible structures from near-source earthquakes since they can provide a controllable rigid-plastic behaviour.

The dynamic response of a structure is a function of its mechanical characteristics and the nature of the induced excitation. Mechanical properties which are desirable to mitigate the structure's response when subjected to certain inputs might amplify its response created from other inputs. Ground motions generated from earthquakes differ from one another on magnitude, source characteristics, distance and direction from the rupture location and local soil conditions. Accordingly, seismic protection strategies should vary with the character of the ground motion. Motions containing high frequencies and sharp accelerations are most detrimental to stiff, low-rise structures but they can be mitigated by base isolation. Long duration excitations

*Assistant Professor

CCC 0098–8847/97/050571–21$17·50

Received 22 March 1996
Revised 27 October 1996

which amplify gradually can be mitigated using passive dampers. However, there are some ground motions that are particularly challenging to accomodate, especially for flexible structures, such as moment-resisting frame buildings or seismically isolated structures. These motions contain large displacement pulses, say one or two pulses from 0·5 to more than 1·0 m with peak velocity of 1·0 m/sec or higher. These large ground displacements can be usually attributed to what seismologists call near-source motions.[2, 3] These motions are the result of stress waves moving in the same direction as the fault rupture, thereby being crowded together to produce a long-duration pulse. The distractive potential of near-source earthquakes to flexible structures has received recently considerable attention by Professor Hall and his coworkers.[4–6]

Figure 1 shows the acceleration, velocity and displacement histories of the 17 January 1994 Northridge earthquake recorded at the LADWP Rinaldi receiving station. This motion resulted in a forward only (non-reversing) ground displacement, that resembles a smooth step function, and a velocity pulse that resembles a finite delta function. Hall *et al.*[5] denoted these forward motions: pulses of type A. Figure 2 shows the acceleration, velocity and displacement histories of the 28 June 1992 Landers earthquakes recorded at the SCE Lucerne Valley station. This motion resulted in a forward and back pulse with a velocity history resembling a single-period-long harmonic motion. Had the negative hump in the velocity history generated the same area than the positive hump the permanent displacement shown in Figure 2 (bottom plot) would have been zero. Hall *et al.*[5] denoted these forward and back motions: pulses of type B. This nomenclature is kept in this paper.

In this paper we first approximate pulse-type A and pulse-type B motions with simple trigonometric functions. Trigonometric functions that describe *cycloidal fronts*[7] are preferred to the square pulses used by Hall *et al.*[5] because they do not induce infinite accelerations or 'jerks' and allow for a simple closed-form solution that describes most of the physics of the problem at hand. Moreover, simple expressions are derived that relate the period of the pulse to the maximum-displacement-to-maximum-velocity ratio. Subsequently, it is shown using a simple mathematical model and its analytical solution, that energy dissipators that exhibit a rigid-plastic (friction-type) behaviour can provide significant protection to base-isolated structures when excited from near-source earthquakes. One- or two-span isolated bridges (overpasses) are typical example of such structures. However, large friction forces are responsible for permanent displacements. Permanent displacements can be avoided by relaxing the friction forces at some time during the free vibration of the structure, while a viscous mechanism is needed to damp free vibrations. This need for adjusting friction-type

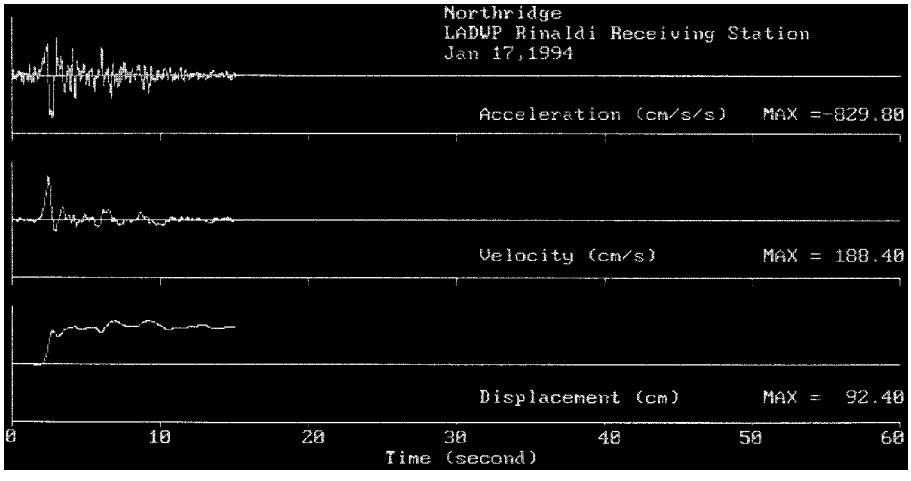

Figure 1. Recorded motions at the Rinaldi station during the 17 January 1994, Northridge earthquake

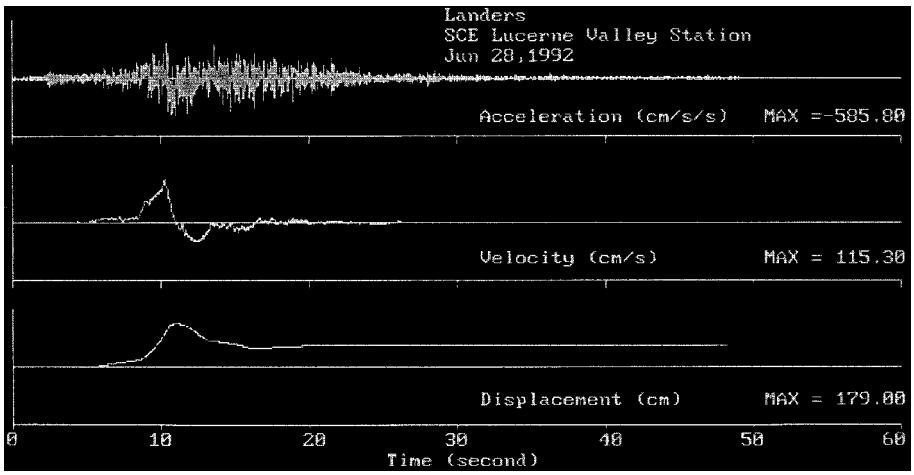

Figure 2. Recorded motions at the Lucerne Valley station during the 28 June 1992, Landers earthquake

forces suggests that electrorheological dampers, or other dissipative devices that can provide a rigid-viscoplastic behaviour, could be a practical solution.

CLOSED-FORM APPROXIMATION OF PULSE MOTIONS

In this paper we are interested to construct an analytical solution to the dynamic response of a SDOF system equipped with dampers which can exhibit behaviour ranging from rigid-plastic to purely viscous. Accordingly, a simple, yet realistic functional expression for the pulse motion is needed. The proposed analytical expressions for the ground acceleration velocity and displacement histories for pulse motions of type A are:

$$a_{gA}(t) = \omega_p \frac{V_p}{2} \sin(\omega_p t), \quad 0 \leqslant t \leqslant T_p \tag{1}$$

$$v_{gA}(t) = \frac{V_p}{2} - \frac{V_p}{2} \cos(\omega_p t), \quad 0 \leqslant t \leqslant T_p \tag{2}$$

$$d_{gA}(t) = \frac{V_p}{2} t - \frac{V_p}{2\omega_p} \sin(\omega_p t), \quad 0 \leqslant t \leqslant T_p \tag{3}$$

where V_p is the amplitude of the velocity pulse and $T_p = 2\pi/\omega_p$ is the predominant period and duration of the pulse. The motion described by equations (1)–(3) is also known as a cycloidal front.[7] The value of T_p can be easily extracted from equations (2) and (3) by dividing the maximum pulse-displacement with the maximum pulse-velocity:

$$\frac{|d_{gA}|_{max}}{|d_{gA}|_{max}} = \frac{T_p}{2} \Rightarrow T_p = 2\frac{|d_{gA}|_{max}}{|d_{gA}|_{max}} \tag{4}$$

Going back to Figure 1 the validity of formula (4) can be established. With $|d_{gA}|_{max} = 92{\cdot}4$ cm and $|v_{gA}|_{max} = 188{\cdot}4$ cm/sec, $T_p \approx 1{\cdot}0$ sec. Indeed, the width of the velocity pulse on the centre plot is about 1.1 sec which is in agreement with the computed value from equation (4). Now, substituting the value of $T_p = 1{\cdot}0$ sec in equation (1), the value for the maximum acceleration that one obtains is $|a_{gA}|_{max} = 590$ cm/sec^2, which is 30 per cent less than the maximum recorded value. However, if one considers that the acceleration record

contains several random spikes, whereas the computed value is obtained by differentiating a smooth function, the prediction is satisfactorily.

For the forward and back pulse-motions of type B the proposed analytical expressions for the ground acceleration, velocity and displacement histories are

$$a_{gB}(t) = \omega_p V_p \sin\left(\omega_p t + \frac{\pi}{2}\right), \quad 0 \leqslant t \leqslant T_p \tag{5}$$

$$v_{gB}(t) = -V_p \cos\left(\omega_p t + \frac{\pi}{2}\right), \quad 0 \leqslant t \leqslant T_p \tag{6}$$

$$d_{gB}(t) = \frac{V_p}{\omega_p} - \frac{V_p}{\omega_p} \sin\left(\omega_p t + \frac{\pi}{2}\right), \quad 0 \leqslant t \leqslant T_p \tag{7}$$

where again V_p is the amplitude of the velocity pulse and $T_p = 2\pi/\omega_p$ is the predominant period and duration of the pulse. Equation (5) is expressed in terms of a sine function because the solution for the response presented later is for a sine excitation. The value of T_p can be easily extracted from equations (6) and (7) by dividing the maximum pulse-displacement with the maximum pulse-velocity:

$$\frac{|d_{gB}|_{max}}{|v_{gB}|_{max}} = \frac{2}{\omega_p} \Rightarrow T_p = \pi \frac{|d_{gB}|_{max}}{|v_{gB}|_{max}} \tag{8}$$

Going back to Figure 2 the validity of equation (8) can be established. With $|d_{gB}|_{max} = 179$ cm and $|v_{gB}|_{max} = 115{\cdot}3$ cm/sec, $T_p = 4{\cdot}87$ sec, which is exactly the time duration of the main pulse shown on the velocity record (centre plot). For equations (4) and (8), one observes that in the case of a forward only (type A) pulse, the pulse duration, T_p, is equal to two times the maximum displacement to maximum velocity ratio, whereas in the case of a forward and back pulse (type B) the pulse duration, T_p, is equal to π times the same ratio. This means that a type-B pulse, will have approximately 1·6 times larger predominant period than a type-A pulse assuming that they have the same maximum displacement to maximum velocity ratio. Another interesting difference in the construction of the analytic expressions that describe type-A and type-B pulses is that in the case of a type-B pulse with maximum velocity equal to V_p, the acceleration amplitude is $\omega_p V_p$, whereas in the case of a type-A pulse with maximum velocity equal to V_p, the acceleration amplitude is $\omega_p V_p/2$.

Figure 3 shows pulse motions of type A (left) computed with equations (1)–(3) and pulse motions of type B (right) computed with equations (5)–(7). In these equations the maximum values of ground velocities and displacements shown in Figures 1 and 2 have been used, respectively.

RIGID-PLASTIC VERSUS VISCOUS BEHAVIOUR

In this section we concentrate on the response of a single-degree-of-freedom (SDOF) oscillator that approximates a stiff superstructure resting on a isolation system. For instance, the response of a one- or a two-span isolated bridge (overpass) oscillating along its longitudinal direction can be approximated with this model. Its equation of motion is

$$\ddot{u}(t) + \omega_0^2 u(t) + \frac{P(t)}{m} = -a_g(t) \tag{9}$$

where $u(t)$ is the relative to the ground displacement history, ω_0 the natural frequency of the isolation system, m the mass of the superstructure, $a_g(t)$ the ground acceleration and $P(t)$ the damping force resulting from the isolation system given by

$$P(t) = 2\xi m\omega_0 \dot{u}(t) + F \operatorname{sgn}[\dot{u}(t)] \tag{10}$$

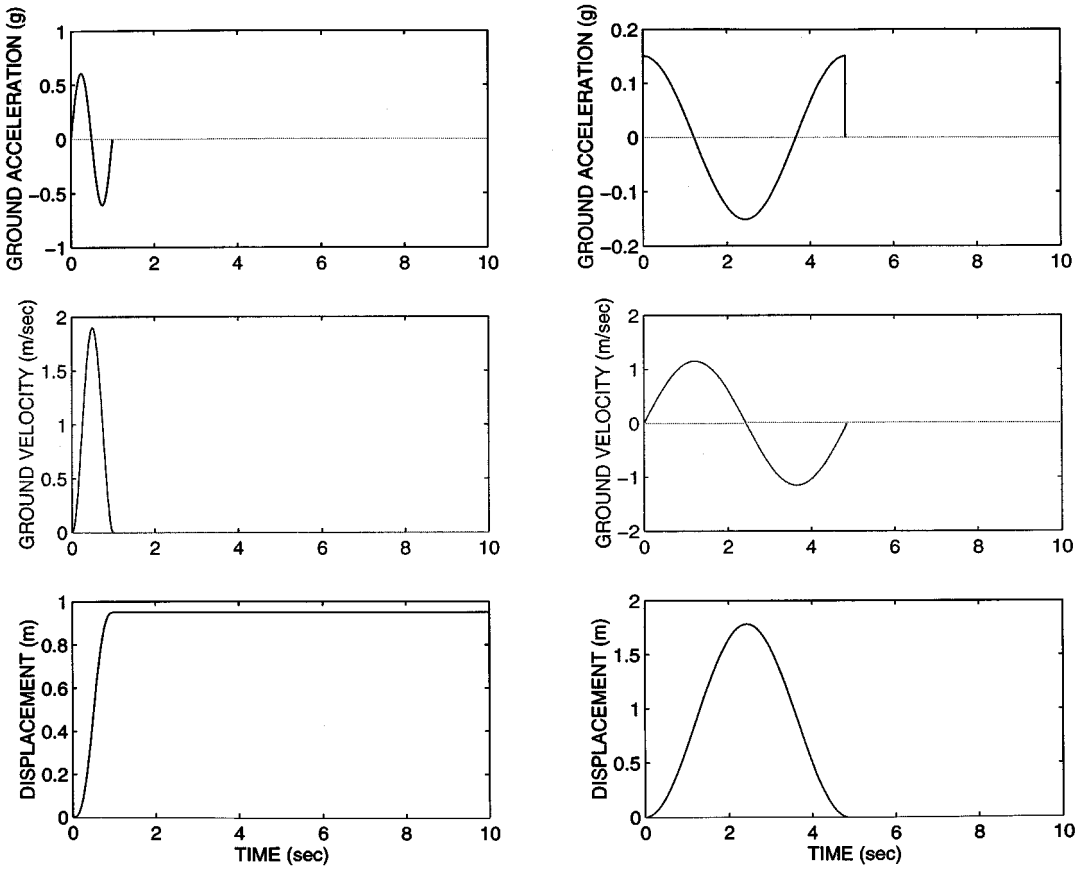

Figure 3. Computed pulse type-A (left) that approximates the recorded motion shown in Figure 1 and pulse type-B (right) that approximates the recorded motion shown in Figure 2

In equation (10), ξ is the viscous damping ratio and F the friction force that results from some friction-type (rigid-plastic) behaviour and will be discussed in the sequel.

The purpose of this section is to examine some of the fundamental differences in the response of the oscillator described by equation (9), when the damping force is either of purely viscous nature ($F = 0$), or of frictional nature. Under harmonic excitation with frequency ω_p, and velocity–response–amplitude, V, the energy dissipated per cycle when the dissipation is viscous only, is

$$E_v = 2\pi\xi m\omega_0 VU \tag{11}$$

where U is the displacement amplitude of the response. When the dissipation is due only to friction (rigid-plastic) forces, the energy dissipated per cycle with the same displacement amplitude U, is

$$E_p = 4FU \tag{12}$$

By defining the plastic damping ratio

$$\varepsilon = j\frac{F}{m\omega_p V_p} \tag{13}$$

the energies dissipated per cycle due to viscous effects given by equation (11), and due to plastic effects given by equation (12) become equal when

$$\varepsilon = j\frac{\pi}{2}\frac{\xi}{\beta}\frac{V}{V_p} \tag{14}$$

in which $\beta = \omega_p/\omega_0$ is the frequency ratio, and $j = 1$ for a type-B pulse and $j = 2$ for a type-A pulse (recall that in the case of a type-B pulse with maximum velocity equal to V_p, the acceleration amplitude is $\omega_p V_p$, whereas in the case of a type-A pulse with maximum velocity equal to V_p, the acceleration amplitude is $\omega_p V_p/2$). According to equation (13), sliding occurs only when $\varepsilon < 1$.

In equation (14), V is the steady-state velocity response amplitude of the SDOF system subjected to a harmonic excitation with frequency ω_p. However, in this study where pulse excitations are of interest steady-state conditions hardly prevail and equation (14) is only an approximate relation between ε and ξ. It has been observed after investigating the response of a variety of SDOF systems that when the pulse frequency, ω_p, is close to the natural frequency, ω_0 (say $0{\cdot}6 < \beta < 1{\cdot}2$), the ratio jV/V_p in equation (14) can be replaced with one, and equation (14) simplifies to

$$\varepsilon \approx \frac{\pi}{2}\frac{\xi}{\beta} \tag{15}$$

Low-period isolation systems

Most isolation periods of base-isolated buildings are between 2 and 3 sec. However, some stiff isolation systems result in isolation periods a low as 0·6 sec. For instance, there is a three-storey braced steel-frame residential building located on Purdue Avenue, Los Angeles, which is supported on helical steel springs and viscoelastic fluid dampers and has a first isolation period of 0·625 sec. The response of this structure excited by the Northridge earthquake has been investigated in detail by Makris and Deoskar.[8] In that study the ground motion that was recorded below the isolators of the building was used, and it was found that bearing displacements probably reached the displacement capacity of the isolation system which is 5·5 cm. Figure 4 shows the recorded accelerations along the SW–NE direction below the isolators of the Purdue-Avenue building (top); the comparison between the computed and recorded accelerations of the building at the first floor (centre) and the computed bearing displacements along the SW–NE and vertical direction (bottom). Luckily, this isolated buildings is located 24 km south–southeast of the Northridge epicentre and survived the Northridge earthquake.

The fault mechanism of the Northridge earthquake in conjunction with the topography of the Greater Los Angeles area was responsible for a variety of ground motions, all being generated from the same seismic event.[6] This variability in ground motions generated from a near-source earthquake suggests that seismic protection of the building environment cannot be achieved with a single technique.

To the south of the epicentre the shaking from the Northridge earthquake was strong but mostly in the form of high frequencies and sharp accelerations for which the seismic isolation concept is beneficial. Indeed, Makris and Deoskar[8] showed that the isolation system of the Purdue-Avenue building reduced the maximum structural acceleration by approximately 45 per cent of the acceleration that the building would have developed, had the building been conventionally founded (no isolation).

Near the epicentre and to the north, motions with longer periods, exhibiting large velocities and displacements, have been recorded. In these areas the isolation system of the Purdue-Avenue building would have been detrimental. Figure 5 plots the relative to the ground displacement and velocity, and absolute acceleration response histories of a SDOF system with isolation period equal to the first isolation period of the Purdue-Avenue building, $T_0 = 0{\cdot}625$ sec, when subjected to the pulse excitation of type A shown on the left of Figure 3. Recall that this excitation is a good approximation of the Northridge motion recorded at the Rinaldi station, some 20 km north of the actual location of the isolated building.

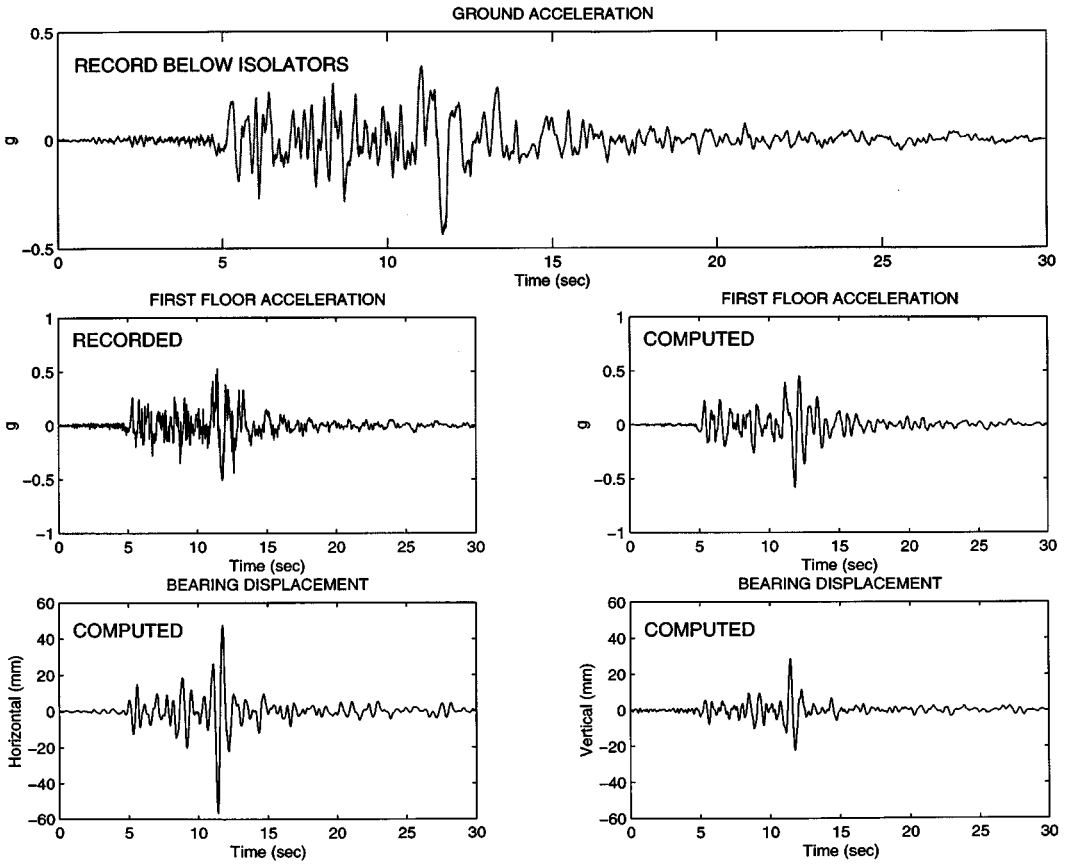

Figure 4. *Top*: Recorded horizontal motion bellow the isolators of the Purdue Aveneue building during the Northridge earthquake. *Centre*: First floor acceleration response. *Bottom*: Computed bearing displacement of the Purdue Avenue building during the Northridge earthquake

The light continuous line in Figure 5 is the response of the SDOF with viscous damping, $\xi = 0{\cdot}234$, which is equal to the first modal damping ratio of the isolated building.[9, 8] In this case the displacement of the bearings exceed 9 cm (near by two times the displacement capacity of the isolation system of the Purdue-Avenue building) and the acceleration is of the order of 1·0 g. Since the Rinaldi station record has been approximated with a cycloidal front the maximum structural response (9·3 cm) can be also obtained from published shock spectra due to pulse type-A excitations.[7]

Consider now the case where in addition to the viscous dampers a device that can deliver friction-type (rigid-plastic) forces is incorporated (later in this paper we will show that electrorheological fluid dampers have the capability of providing both viscous and friction-type forces). The heavy solid line in Figure 5 is the response of the SDOF system with $\xi = 0{\cdot}234$ and $\varepsilon = 0{\cdot}50$. The zero-velocity segments along the response of the isolated structure with friction-type dampers are due to finite sticks of the superstructure. The analytical solution of the equation of motion when friction-type dampers are used and the detection of the sticking mode is discussed in the next section. The additional friction-type forces to the existing viscous forces reduced the bearing displacement from 9·3 to 5·0 cm which is less than the displacement capacity of the isolation system of the Purdue-Avenue building. It is interesting to note that while friction-type forces reduce drastically the maximum displacement they are responsible for the permanent displacement of the

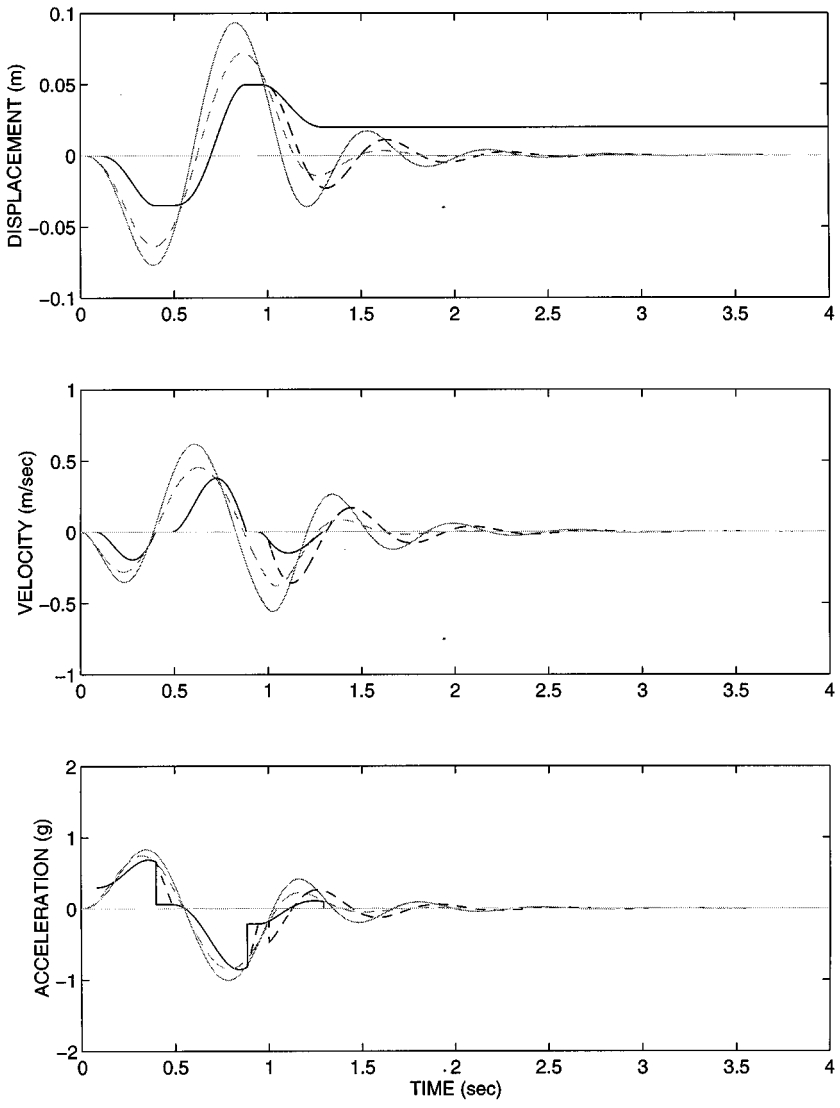

Figure 5. Computed response of a SDOF system with $T_0 = 0{\cdot}625$ sec subjected to the pulse type-A motion shown in Figure 3, left. Light solid line: viscous damping only ($\xi = 0{\cdot}234$, $\varepsilon = 0{\cdot}0$). Heavy solid line: Viscous damping is combined with friction-type damping ($\xi = 0{\cdot}234, \varepsilon = 0{\cdot}50$). Light dahsed line: $\xi = 0{\cdot}434, \varepsilon = 0{\cdot}0$. Equivalent viscous damping was computed with equation (15). Heavy dashed line: Same as heavy solid line but $\varepsilon = 0{\cdot}0$ during free vibrations

superstructure. The use of electrorheological dampers can eliminate this problem. The heavy dashed line shows the response of the building when the friction-type forces are removed at the end of the pulse excitation, whereas viscous forces are kept. Although this is an elementary way of controlling the structural response, Figure 5 demonstrates that an adjustable combination of friction and viscous forces can provide optimum structural response. A systematic strategy for controlling the response of structures equipped with controllable fluid dampers is under development.[10]

With the help of equation (15) the additional plastic damping ratio with $\varepsilon = 0{\cdot}5$ corresponds to an additional viscous-damping-ratio value of 0·2, which together with the initial viscous-damping-ratio value

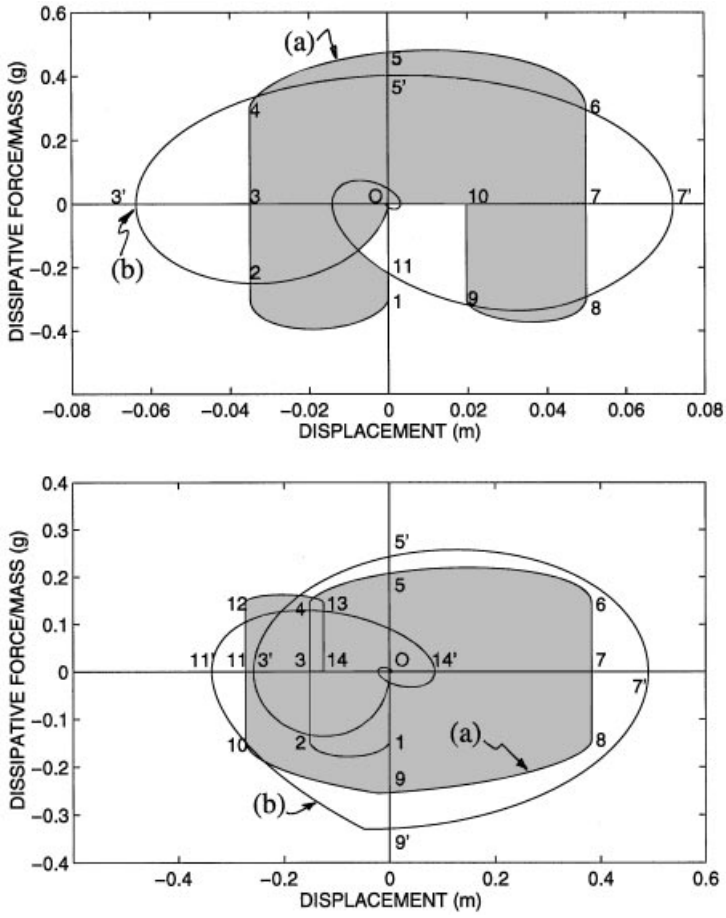

Figure 6. Dissipative force–displacement trajectories. Top: Response of SDOF due to the pulse type-A motion shown in Figure 3, left. Trajectory (a) is obtained with viscous damping, $\xi = 0{\cdot}234$ and plastic damping, $\varepsilon = 0{\cdot}5$; trajectory (b) is obtained with equivalent viscous damping only, $\xi = 0{\cdot}434$. Bottom: Response of SDOF due to the pulse type-B motion shown in Figure 8. Trajectory (a) is obtained with viscous damping, $\xi = 0{\cdot}15$ and plastic damping, $\varepsilon = 0{\cdot}4$; trajectory (b) is obtained with equivalent viscous damping only, $\xi = 0{\cdot}4$

0·234, adds up to $\xi = 0{\cdot}434$. The light dashed line in Figure 5 is the response of the SDOF with viscous damping ratio $\xi = 0{\cdot}434$ and $\varepsilon = 0$. Despite the large amount of viscous damping, the bearing displacements exceed 7 cm (which is more than the 5.5 cm displacement capacity of the isolation system of the Purdue-Avenue building), and the resulting velocities are also larger than the resulting velocities computed when the initial viscous damping was enhanced with friction-type damping (heavy lines).

Figure 6 (top) compares the dissipative force–displacement trajectories of the SDOF system when: (a) the initial viscous damping, $\xi = 0{\cdot}234$, is combined with additional plastic damping, $\varepsilon = 0{\cdot}5$ and (b) the additional plastic damping is converted to equivalent viscous damping $\xi = 0{\cdot}434$. It is interesting to note that although in case (b) the energy dissipated during the first cycle (area under 0–2–3′–4–5′–6–7′–8–9–11) is slightly more than the energy dissipated in case (a) (shaded area), the maximum displacement in case (b) is 50 per cent larger than in case (a). Moreover, both dissipative configurations result in substantial base shears that exceed 40 per cent the weight of the structure, which shows that supplemental damping reduces displacements at the expense of developing substantial base shears.

From the above comparisons one can clearly recognize that for these rapid, long period motions, viscous damping alone has little effect in reducing the response, whereas, friction-type damping can substantially reduce displacements and velocities without increasing accelerations. On the other hand, viscous damping alone is beneficial when high-frequency motions with sharp accelerations, like the one shown in Figure 4, excite the structure. This strong need for adjusting the type of dissipation mechanism in order to protect a structure from two totally different motions that were generated from the same earthquake only some 20 km apart, shows that semiactive dampers can be a promising alternative to protect effectively structures from major earthquakes.

Long-period-isolation systems

As we discuss earlier, a major concern in the design of a base-isolated structure is to accommodate large displacements across the isolators which could occur during strong long period motions generated from major earthquake. Typically, the maximum bearing displacement, D_{TM} (total maximum displacement in the UBC[11]), of buildings resting on elastomeric bearings is of the order of $D_{TM} = 40$ cm, while $D_{TM} = 60$ cm is about the largest that is currently being used for design locations near major faults. A typical value of an isolation period is $T_0 = 2{\cdot}25$ sec.

The Lucerne Valley Station record from the Landers earthquake shown in Figure 2 is of particular interest since the predominant period of the input, $T_p = 4{\cdot}85$ sec, is more than two times the typical value of isolation periods ($T_0 = 2{\cdot}0$–$2{\cdot}25$ sec). From published shock spectra on the response of a SDOF system subjected to a forward and back pulse,[7] the displacement response amplifies significantly for values of $T_p/T_0 < 2$. Accordingly, an isolated structure with isolation period, $T_0 = 2{\cdot}25$ sec would have survived the Landers earthquake because the predominant period of the Lucerne Valley Station record is so unusually large ($T_p = 4{\cdot}85$ sec). Had the predominant period of the motion been shorter (say $T_p < 1{\cdot}6T_0$) the relative displacement of the superstructure would have been of the order of 1 m or more.[7]

Not every pulse motion from a near-source earthquake is either of type A or type B. Figure 7 shows the acceleration, velocity, and displacement histories of the 17 January 1994 Northridge earthquake recorded at the LADWP Sylmar Conveter Station. This motion has elements of both a type-A and a type-B motion. Had the first positive velocity hump been more substantial the motion would have been closer to a type-B pulse. It is interesting to note, however, that equation (8) provides a dependable estimate of the predominant period of the motion. With $|d_g|_{max} \approx 100$ cm and $|v_g|_{max} \approx 130$ cm/sec, $T_p = 2{\cdot}4$ sec which is good estimate of the

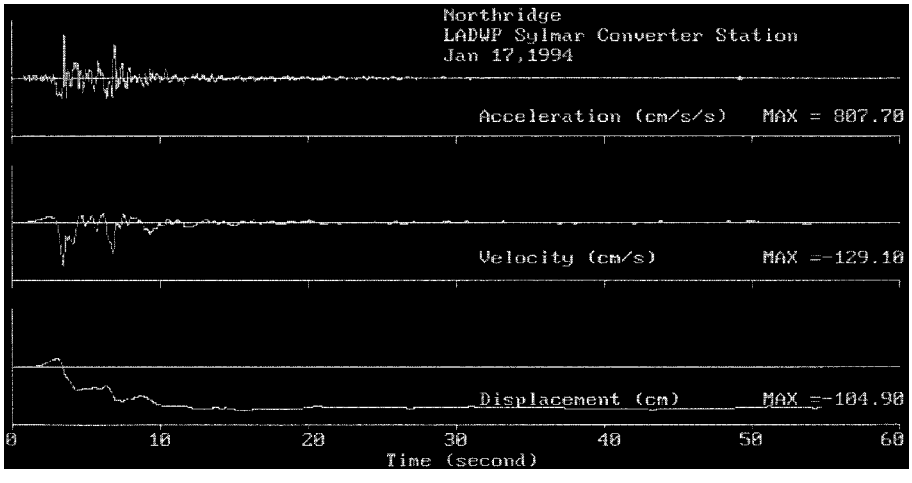

Figure 7. Recorded motions at the Sylmar Converter station during the 17 January 1994, Northridge earthquake

duration of each of the two strong velocity pulses that one observes on the centre plot of Figure 7. Note that now the predominant period of the pulse, $T_p = 2{\cdot}4$ sec, is much closer to the isolation period of the structure, $T_0 = 2{\cdot}25$ sec, and this will amplify drastically the response.

In order to demonstrate the advantage of having controllable fluid dampers in an seismic isolation system, consider the case of a type-B pulse with $|d_{gB}|_{max} = 95$ cm and $|v_{gB}|_{max} = 130$ cm/sec. Figure 8 show the displacement, velocity and acceleration histories of the pulse. The characteristics of this motion are typical characteristics of a motion expected from a near-source earthquakes and resemble the characteristics of the recorded motion shown in Figure 7. The corresponding predominant period of this motion is, $T_p = 2{\cdot}3$ sec.

Figure 9 shows relative to the ground displacement, velocities and acceleration response histories of a SDOF isolated structure with isolation period, $T_0 = 2{\cdot}25$ sec, when subjected to the pulse excitation of

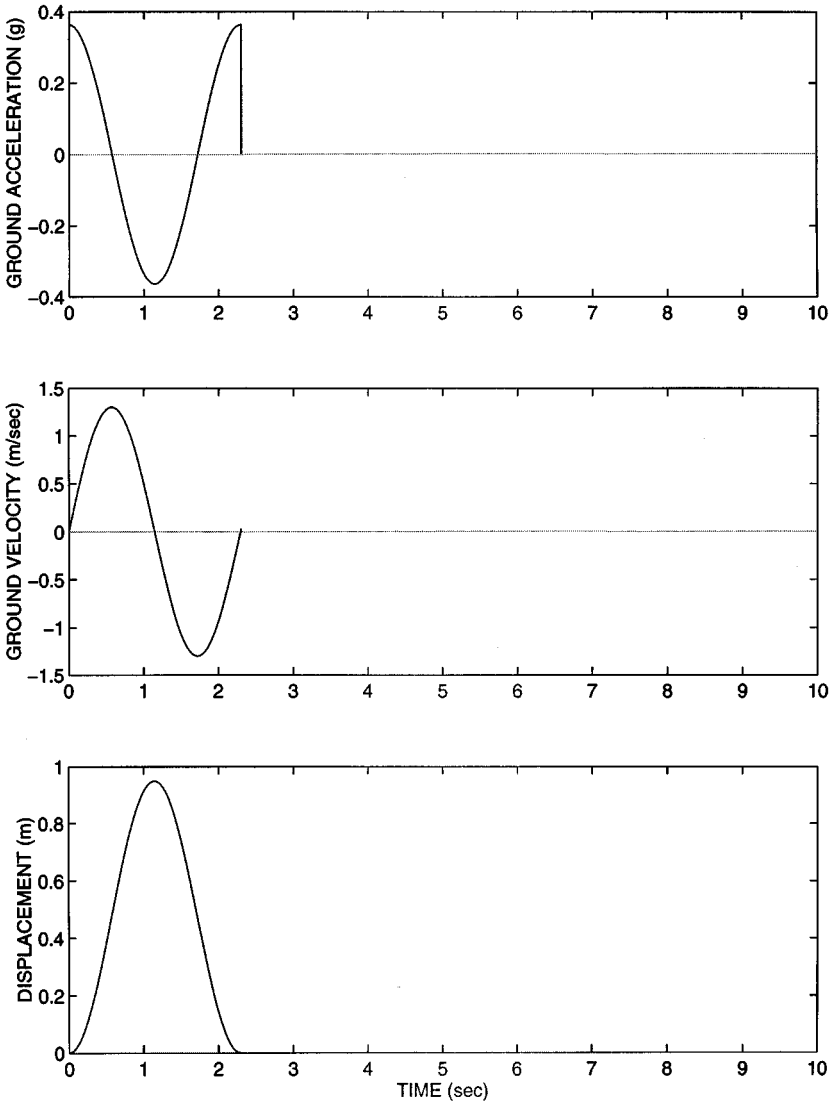

Figure 8. Typical pulse type-B motion from a near-source earthquake

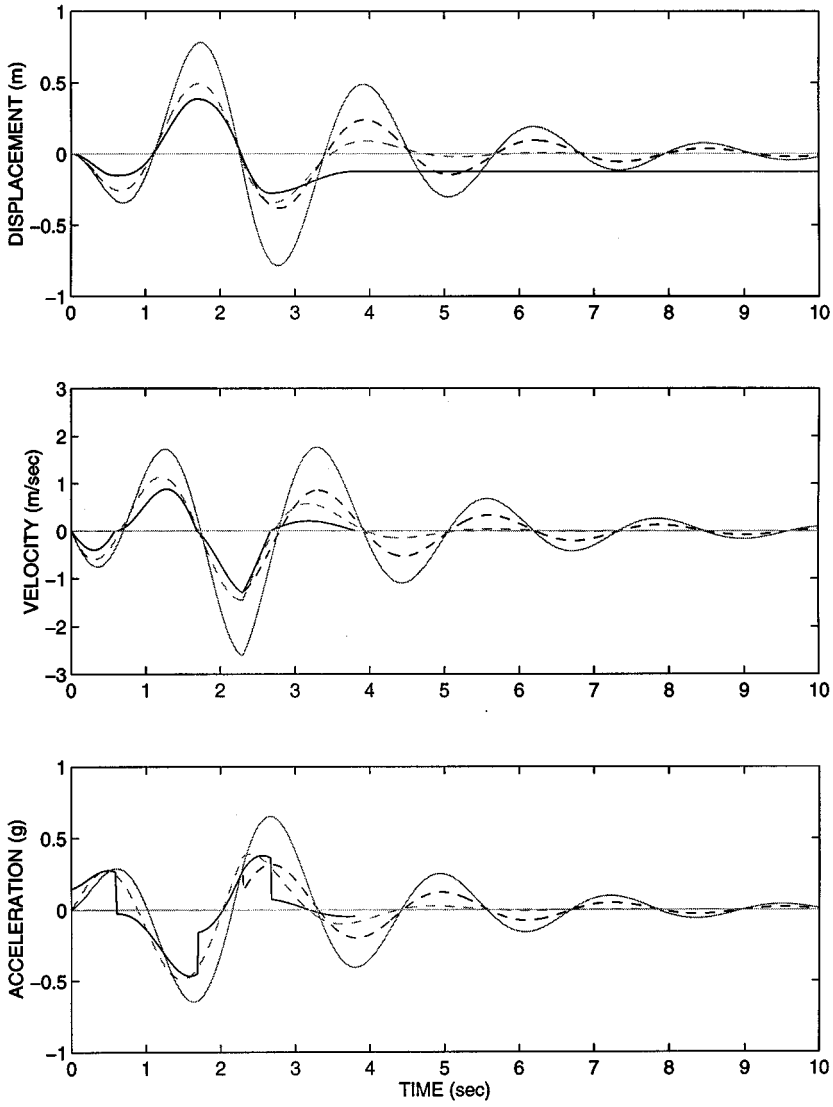

Figure 9. Computed response of a SDOF system with $T_0 = 2{\cdot}25$ sec subjected to the pulse type-B motion shown in Figure 8. Light solid line: viscous damping only ($\xi = 0{\cdot}15$, $\varepsilon = 0{\cdot}0$). Heavy solid line: Viscous damping is combined with friction-type damping ($\xi = 0{\cdot}15$, $\varepsilon = 0{\cdot}40$). Light dashed line: $\xi = 0{\cdot}40$, $\varepsilon = 0{\cdot}0$. Equivalent viscous damping was computed with equation (15). Heavy dashed line: Same as heavy solid line but $\varepsilon = 0{\cdot}0$ during free vibrations

type-B shown in Figure 8. The light continuous line in Figure 9 is the response of the SDOF with viscous damping, $\xi = 0.15$, which is a typical value of equivalent viscous damping for an isolation system. In this case the bearing displacements reach 80 cm, which is 1·5–2 times the value of the clearance gap. Velocities and accelerations are also very large. The heavy solid line in Figure 9 is the response of the SDOF system with $\xi = 0{\cdot}15$ and $\varepsilon = 0{\cdot}40$. The additional friction-type forces to the existing viscous forces reduced the bearing displacement from 80 to 38 cm which is within the displacement capacity of the isolation system. Again, although the presence of a friction-type force reduced drastically the maximum displacement, it is responsible for the presence of a permanent displacement.

According to equation (15) the additional plastic damping ratio of $\varepsilon = 0{\cdot}4$ corresponds to an additional viscous-damping-ratio value of 0·25, which together with the initial viscous-damping-ratio value 0·15, adds up to $\xi = 0{\cdot}4$. The light dashed line in Figure 9 is the response of the SDOF with viscous damping ratio $\xi = 0{\cdot}4$ and $\varepsilon = 0$. Despite the large amount of viscous damping, the bearing displacements are of the order of 50 cm which is 30 per cent more than the displacement obtained with friction-type damping forces. Once again the need of having a controllable damping device is clear. Before the pulse strikes the structure, friction-type forces are activated to reduce displacements without increasing accelerations. At some point friction forces are relaxed to allow the structure to recentre while free vibrations are damped by virtue of viscous damping.

Figure 6 (bottom) compares the dissipative force–displacement trajectories of the SDOF system when: (a) the initial viscous damping, $\xi = 0{\cdot}15$, is combined with additional plastic damping, $\varepsilon = 0{\cdot}4$ and (b) the additional plastic damping is converted to equivalent viscous damping $\xi = 0{\cdot}40$. It is interesting to note that although in case (b) the energy dissipated during the first two cycles (area under 0–2–3′–4–5′–7′–9′–10–11′–13–14′) is more than the energy dissipated in case (a) (area under 0–1–2–3–4–5–6–7–8–9–10–11–12–13–14), the maximum displacement in case (b) is 30 per cent larger than in case (a). This shows again that in the case of pulse excitations hysteretic dissipation is more attractive than its equivalent viscous.

The presence of friction-type forces are beneficial in mitigating the response of SDOF systems such as short overcrossings or other stiff superstructures supported on a flexible isolation system. In the case of a MDOF structure such as a multi-storey building, the presence of substantial friction forces at the isolation level might reduce base displacements but will transfer the induced energy to higher vibration modes of the superstructure. A numerical study on a three-storey base-isolated building supported on flexible bearings and subjected to the 1994 Sylmar record and another simulated event has been presented by Hall *et al.*[5]

ANALYSIS OF RESPONSE WITH COULOMB FRICTION

In this section we present the solution of the equation of motion of a SDOF with combined viscous and Coulomb-friction damping subjected to a sinusoidal excitation. For a harmonic acceleration input and a dissipative force given by equation (10), the equation of motion given by equation (9) takes the form

$$\ddot{u}(t) + 2\xi\omega_0\dot{u}(t) + \omega_0^2 u(t) + \frac{F}{m}\operatorname{sgn}[\dot{u}(t)] = -A_p \sin(\omega_p t + \phi) \tag{16}$$

in which A_p is the acceleration amplitude of the pulse motion. Recall that for a pulse type-A motion, $A_p = \omega_p V_p/2$, whereas for a pulse type-B motion, $A_p = \omega_p V_p$.

The signum function of the velocity history makes equation (16) a nonlinear equation and its solution results in stops with finite duration. A detailed study on the solution of equation (16) accounting for multiple stops has been presented by Makris and Constantinou.[12] Readers who are interested in the logical procedure to detect a stop and evaluate its duration are referred to Reference 16. Herein only the solution for the displacement history is presented:

$$u(t) = e^{-\xi\omega_0 t}(A_1 \cos\omega_d t + A_2 \sin\omega_d t) + \frac{F}{m\omega_0^2} - \beta\frac{V_p}{\omega_p} D[(1-\beta^2)\sin(\omega_p t + \phi) - 2\xi\cos(\omega_p t + \phi)], \quad \dot{u}(t) \leqslant 0 \tag{17}$$

and

$$u(t) = e^{-\xi\omega_0 t}(A_3 \cos\omega_d t + A_4 \sin\omega_d t) - \frac{F}{m\omega_0^2} - \beta\frac{V_p}{\omega_p} D[(1-\beta^2)\sin(\omega_p t + \phi) - 2\xi\beta\cos(\omega_p t + \phi)], \quad \dot{u}(t) > 0 \tag{18}$$

where

$$\omega_d = \omega_0(1 - \xi^2)^{1/2} \tag{19}$$

and

$$D = \frac{1}{(1 - \beta^2)^2 + (2\xi\beta)^2} \tag{20}$$

The integration constants are expressed in terms of general initial conditions, $u(0) = U_0$, and $\dot{u}(0) = \dot{U}_0$, in which the time is equal to zero at the start of each of the subintervals, $\dot{u}(t) > 0$ and $\dot{u}(t) < 0$. Accordingly,

$$A_1 = U_0 + \beta\frac{V_p}{\omega_p}D[(1 - \beta^2)\sin\phi - 2\xi\beta\cos\phi] - \frac{F}{m\omega_0^2} \tag{21}$$

$$A_2 = \beta^2\frac{V_p}{\omega_p}D[(1 - \beta^2)\cos\phi - 2\xi\beta\sin\phi] + \frac{\xi}{\sqrt{1 - \xi^2}}A_1 \tag{22}$$

$$A_3 = U_0 + \beta\frac{V_p}{\omega_p}D[(1 - \beta^2)\sin\phi - 2\xi\beta\cos\phi] + \frac{F}{m\omega_0^2} \tag{23}$$

$$A_4 = \beta^2\frac{V_p}{\omega_p}D[(1 - \beta^2)\cos\phi - 2\xi\beta\sin\phi] + \frac{\xi}{\sqrt{1 - \xi^2}}A_3 \tag{24}$$

Equations (17) and (18) together with the conditions of separation and reattachment are pieced together over each subinterval (of no motion and of motion with reversal of the velocity sign) to construct the entire time history of transient motion. Time histories of velocity and acceleration are determined from equations (17) and (18) by direct differentiation with respect to time. The conditions of separation and reattachment (stop) have been discussed in detail in Reference 16. As the ground motion strikes the structure the mass is in motion. Assuming that the ground moves to the positive displacements the motion of the structure is initially described with equation (17). Stepping through time, a zero-velocity point is reached. Just prior to this point, the excitation, restoring, frictional and inertia forces are determined. According to the magnitude of these forces, the mass will either continue its motion, or come to a stop with finite duration. The duration of the stop depends on: whether the magnitude of the ground acceleration is increasing or decreasing, on whether the magnitude of the restoring force is larger or smaller than the friction force; and whether the amplitude of the inertia forces prior to the stop is larger or smaller than the friction force. All these checks results to a sophisticated flowchart similar to the one presented in Reference 16.

CAN ELECTRORHEOLOGICAL DAMPERS PROVIDE A SOLUTION?

In the foregoing analysis it was shown that seismic protection devices which provide a combination of viscous and adjustable friction-type forces can protect effectively base-isolated structures from rapid, long-period ground motions.

Within the context of seismic protection, studies on controllable friction have been conducted mainly on hybrid sliding-isolation systems. Among others, Feng *et al.*[13] proposed a hybrid isolation systems by modifying the pressure in a fluid chamber incorporated within the isolation bearings, while Yang *et al.*[14] improved the response of a three-storey scale structure supported on sliding bearings by correcting the motion at the base of the structure with a hydraulic actuator. The aforementioned studies invariably involve sophisticated hydraulics including servovalves and considerable power to pressurize oil.

Herein we propose to induce friction-type forces using electrorheological fluid dampers (ER-dampers). ER-dampers, or other controllable fluid dampers,[15] are very attractive since they can operate as passive devices in the absence of power, while they can provide optimum response with a minimum amount of power

which can be supplied through a battery. They are a natural extension of passive fluid dampers, which have been already implemented in conventionally isolated structures and their technology has been tested extensively. As an example, a major application in the US of additional passive fluid dampers combined with elastometric bearings is in the under construction new San Bernandino County Medical Center.[16] The hospital is seismically isolated and the 184 fluid dampers are placed at the isolation level in parallel with high-damping elastomeric bearings.

Electrorheological dampers have attracted considerable attention in the last decade for vibration control of mechanical and structural systems. Early studies by Stevens *et al.*,[17] showed how a simple ER-damper is capable of reducing displacement amplitudes when electric field is applied, while Duclos[18] has reported on various applications that ER-dampers have found in the automotive industry. Recently, ER-dampers received considerable attention for vibration control of civil structures. The attraction of ER-dampers is that they are relatively inexpensive compared to hydraulic dampers with mechanically controlled orificing. Ehrgott and Masri,[19] presented identification techniques to model the behaviour of a mall ER-damper that

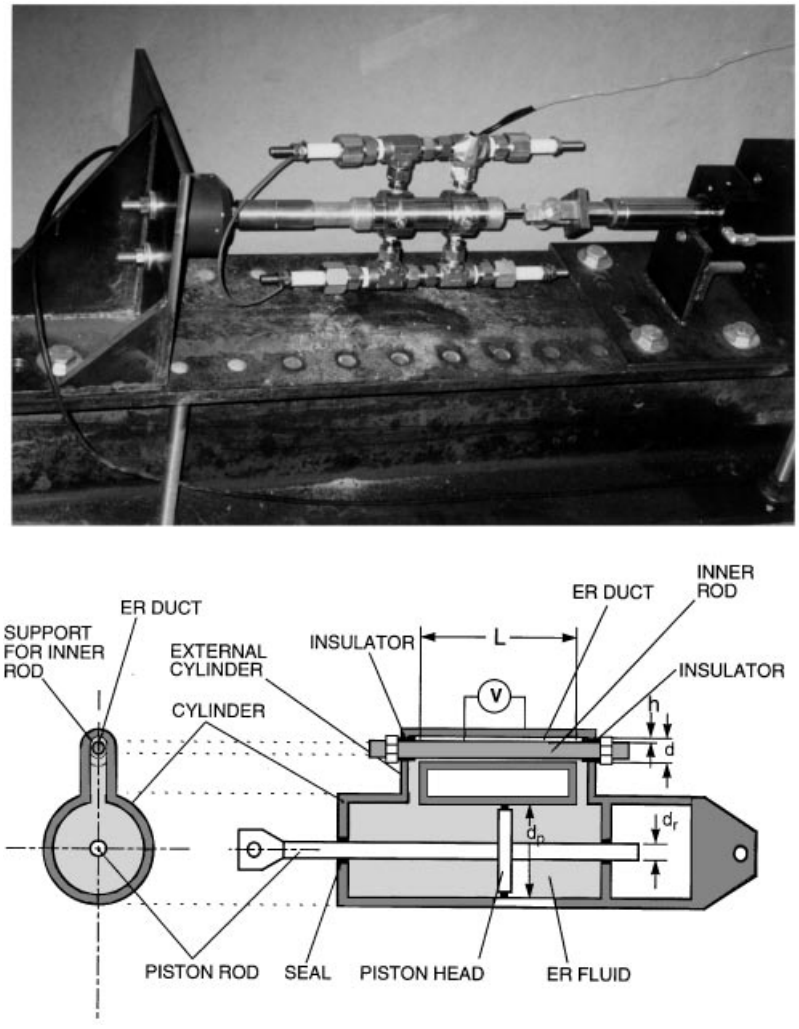

Figure 10. Top: View of constructed electrorheological damper. Bottom: Schematic of the ER-damper

operates under shear flow. Gavin and Hanson[20] designed and tested an ER-damper that consists of a rectangular container and a moving plunger comprised on nine flat parallel plates which are rigidly interconnected.

Most of the ER-dampers proposed in the past involve shear flow. Figure 10 (top) is a photograph of an ER-damper designed by the author and his coworkers.[21] The Hagen–Poiseuille flow that develops within the damper is responsible for the development of large forces across the piston head. A schematic of the damper and the construction of the bypass is shown in Figure 10 (bottom). The damper consists of an outer cylinder and a double-ended piston rod that pushes the ER-fluid through a stationary annular duct. The electric field is created perpendicular to the fluid flow across the bypass. Some of the advantages of the developed ER-dampers shown in Figure 10 are: (1) There are no moving parts within the damper besides the piston. (2) It is a compact device that can produce relatively large forces. (3) The yield forces that ER-dampers exhibit, can provide significant rigidity and when the yield forces are exceeded they can dissipate substantial energy. (4) Once the power fails the damper operates as a passive device that provides a reasonable amount of damping. (5) The damper can operate in a passive state during many seismic events where viscous damping alone is sufficient to mitigate the response. (6) The proposed damper can be positioned in any direction as opposed to other dampers which have to be positioned horizontally due to the presence of a free surface. (7) Settling of the ER-fluid was never a problem in the response of our damper. Even when the damper has been inactive for more than 10 weeks, it responded in a consistent manner as in previous tests. Possible reason for this good performance is that ER-material is nested within a very thin ring (see Figures 10 and 11), and apparently the surface tension that develops on the fluid eliminated the settling problem.

Figure 11 shows a cross-section of the bypass which consists of the inner rod (electrode) and the outer cylinder (ground). One can easily show that the shear stress that develops across the bypass is given by[21]

$$\tau_{xr}(r) = \Delta p \frac{r}{L} \tag{25}$$

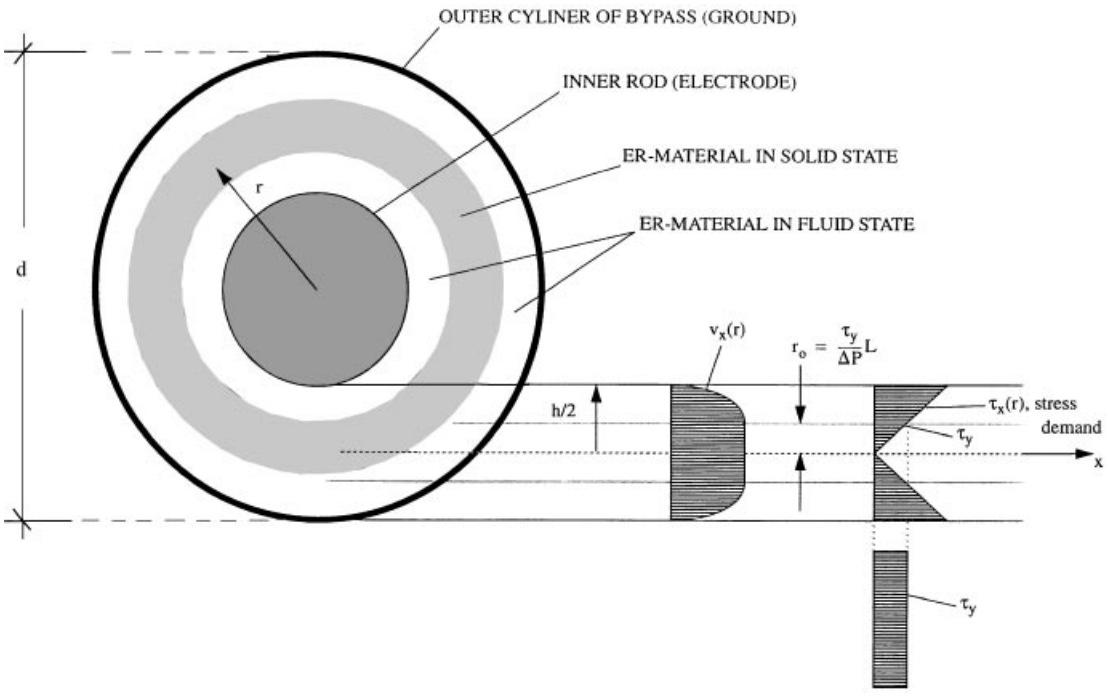

Figure 11. Stress and velocity profiles of the yielding ER-fluid across the annular duct

where Δp is the pressure drop across the piston head, r is the radial distance from centre line of the ER-duct, and L is the length of the duct (see Figure 10). The stress distribution given by equation (25) is independent of the material that flows and can be understood as the stress *demand* across the duct to maintain equilibrium. In the case where $h \ll d$, the solution for the Poisseuille flow between concentric cylinders collapses to that for flow between parallel plates. For instance, if the fluid that flows through is Newtonian, with zero-shear-rate viscosity, η_0, the pressure drop due to viscous stresses under steady flow is given by

$$\Delta p_v = \frac{1}{n}\frac{12\eta_0 LQ}{\pi d h^3} \tag{26}$$

where Q is the flow rate through the ER-duct, d is the diameter of the ER-duct, h is the width of the gap and n is the number of bypasses. Equation (26) express the pressure drop in the case of no field ($E = 0$).

When electric field is applied the behaviour of the ER-fluid is viscoplastic and the shear stress $\tau_{xr}(r)$ has to exceed the finite 'yield' stress, τ_y, to initiate flow. This value of the 'yield' stress can be also understood as the *capacity* of the material to exist in a solid state. If the stress demand, $\tau_{xr}(r)$, given by equation (25) exceed the capacity of the ER-material, τ_y, then the ER-material adjacent to the walls will yield and flow. For a rigid-viscoplastic material the velocity profiles across these 'fluidized' rings is parabolic, whereas the velocity profile across the remaining solid core-ring is constant. From equation (25) one immediately recognizes that as the pressure drop increases, more material yields. The pressure drop under viscoplastic flow is given by[21, 22]

$$\Delta p = \frac{1}{n}\frac{12\eta_0 LQ}{\pi d h^3}\frac{1}{1 - 3\dfrac{\tau_y}{\Delta p}\dfrac{L}{h} + 4\left(\dfrac{\tau_y}{\Delta p}\right)^3\left(\dfrac{L}{h}\right)^3} \tag{27}$$

As flow rate increases, equation (27) reaches asymptotically the expression

$$\Delta p(t) = \frac{P(t)}{A_p} = \frac{1}{n}\frac{12\eta_0 LA_p}{\pi d h^3}\dot{u}(t) + \frac{3L\tau_y}{h}\operatorname{sgn}[\dot{u}(t)] \tag{28}$$

where A_p is the area of the piston head and the flow rate, $Q = A_p\dot{u}(t)$. Equation (28) is valid everywhere but the zero-velocity limit where the factor, three, in the second term reduces to two.

Figure 12 shows recorded (left) and predicted (right) force–displacement loops without electric field ($E = 0$) and with $E = 3$ kV/mm. As the piston velocity increases, viscous effects dominate over plastic effects and the fraction of the force that can be controlled reduces. The predicted response shown on the right of Figure 12 is computed with

$$P(t) = \Delta p(t)A_p + P_y \operatorname{sgn}[\dot{u}(t)], \tag{29}$$

where P_y is a permanent friction force acting on the damper seals and A_p is the area of the piston head. Δp is the pressure drop across the piston head given by equation (27) or (28). Substitution of equation (28) into equation (29) gives

$$P(t) = \frac{1}{n}\frac{12\eta_0 LA_p}{\pi d h^3}A_p\dot{u}(t) + \left[\frac{3L\tau_y}{h}A_p + P_y\right]\operatorname{sgn}[\dot{u}(t)] \tag{30}$$

Equation (30) is the resulting piston force as a function of the piston velocity, the mechanical properties of the ER-material and the geometric characteristics of the damper, and is of the form of equation (10). The first term in equation (30) represents the dissipative forces due to the viscous behaviour of the ER-fluid, while the second term represents the dissipative forces due to the plastic behaviour (friction).

In order to have an effective ER-damper the viscous forces that develop have to be comparable with the plastic forces. When ER-dampers are incorporated within the frame of a flexible structure the design piston velocities are relatively low ($\dot{u} = 3$–10 in/sec), and the design of the damper shown in Figure 10 is appropriate.[21] As the piston velocity increases the number of bypasses has to increase to keep the flow rate at low

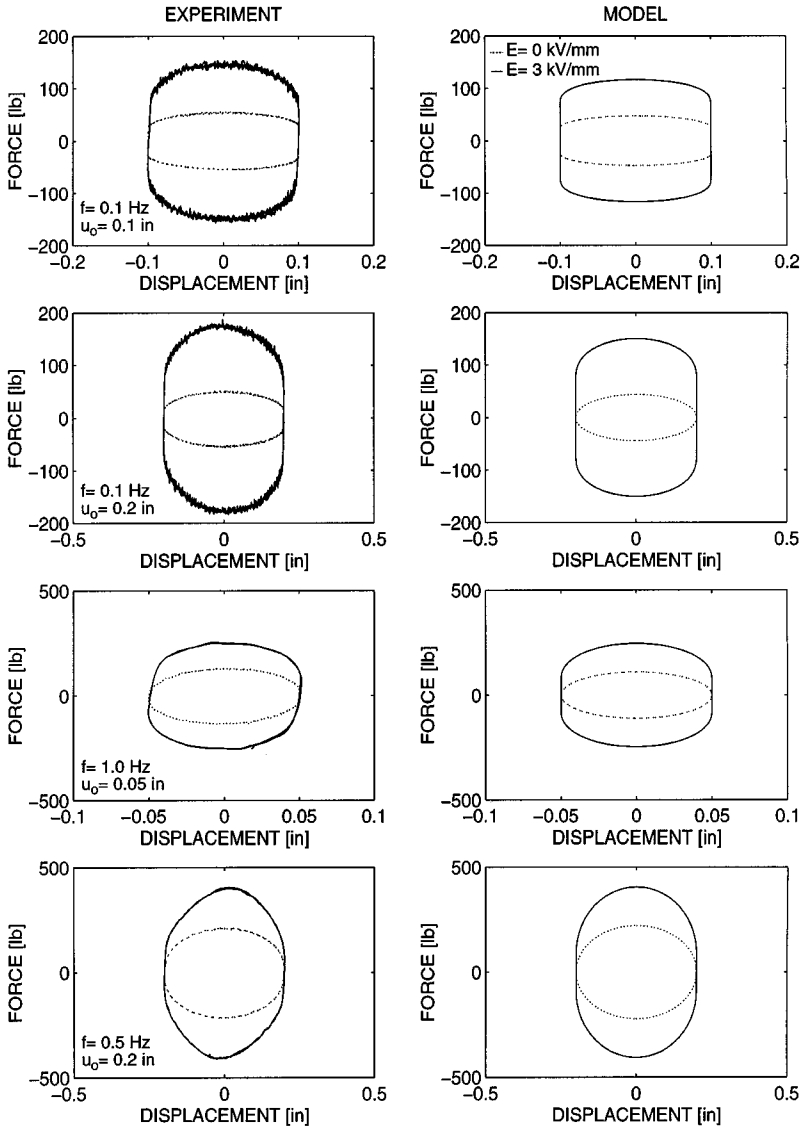

Figure 12. Comparison of recorded and predicted force-displacement loops of the electrorheological damper with ($E = 3$ kV/mm) and without electric field. $\tau_y = 1{\cdot}8$ kPa, $\eta_0 = 7$ Pa sec, $L = 54{\cdot}6$ mm, $d = 14{\cdot}3$ mm, $h = 0{\cdot}8$ mm, $d_p = 33{\cdot}4$ mm, $d_r = 11{\cdot}25$ mm. (1 lb = 4·448 N, 1 in = 25·4 mm)

values. The ER-damper shown in Figure 10 has been designed to accommodate up to four bypasses. When the ER-dampers are placed at the isolation system of the structure the design piston velocities are of the order of 40 in/sec or higher. For this application a different design is needed.

For a cylindrical piston, $A_p = \pi(d_p^2 - d_r^2)/4$, where d_p is the piston-head diameter and d_r is the piston-rod diameter. With the help of equation (13), equation (28) yields the relation between the plastic damping ratio, ε, and viscous damping ratio, ξ:

$$\frac{\varepsilon}{\xi} = \frac{2j\tau_y dh^2\omega_0}{\eta_0(d_p^2 - d_r^2)V_p\omega_p} \tag{31}$$

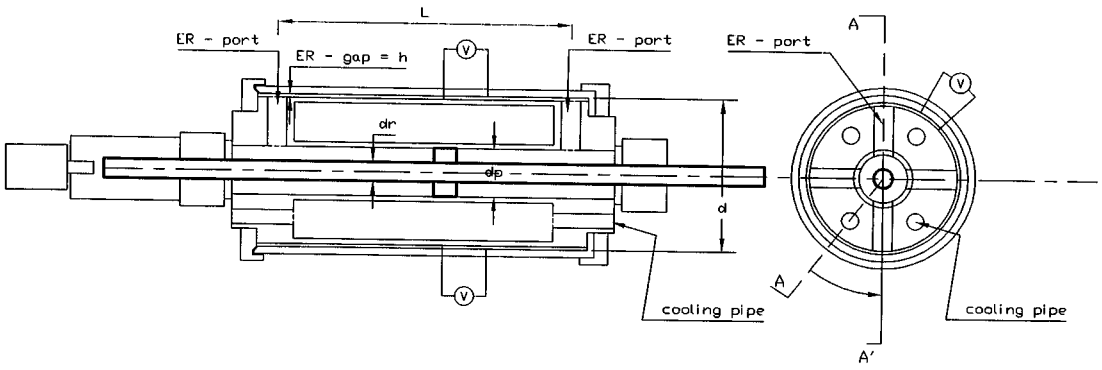

Figure 13. Schematic of the new ER-damper which can operate under high design velocities, adequate for seismic isolation systems. Section A–A is projected in line A–A′

Equation (31) relates the ratio of plastic to viscous damping with the material properties of the ER-fluid to be used, the dimensions of the damper and the parameters of the earthquake pulse. As an example, using the values of $\xi = 0{\cdot}15$ and $\varepsilon = 0{\cdot}40$ which are needed to mitigate the response of the SDOF plotted in Figure 9, the ratio $\varepsilon/\xi = 2{\cdot}67$. With a value of yield stress, $\tau_y = 2$ kPa, $\eta_0 = 0{\cdot}3$ Pa sec, $h = 2$ mm, $d_p = 0{\cdot}085$ m, $d_r = 0{\cdot}030$ m, $\beta = 1$ and $V_p = 1$ m/sec, the value of the diameter of the ER-duct needed is approximately $d = 0{\cdot}30$ m. This design is feasible by creating one concentric ring surrounding the main cylinder of the damper as shown in Figure 13. A new ER-damper based on the concept shown in Figure 13 is under design and its construction and testing is scheduled to be completed before the end of 1997. A damper with a diameter of 0·3 m or even 0·4 m can be easily accommodated in a isolation system, since the clearance of the isolation space is dictated from the height of the bearing. For instance, the height of the high-damping-rubber bearings in the isolation system of the San Bernandino County Medical Center is 0·5 m (20 in). Another attractive feature of the design proposed for the new ER-damper shown in Figure 13 is that the ER-duct has a large contact area with the environment which allows better cooling of the ER-damper. For other applications, where dampers are expected to operate for long time intervals such as wind applications, the new design allows to accomodate internal cooling in the ER-damper. The chamber for internal cooling is shown in Figure 13 at the lower part of the cross-section.

Equation (31) shows that the higher the yield stress of the fluid, the smaller the diameter of duct needed to achieve the same ratio, ε/ξ. A different type of controllable fluids with similar rheologicl behaviour to the ER-fluids but with higher yield stress are magnetorheological fluids (MR-fluids).[15, 23] Although MR-fluids are at an earlier research stage than ER-fluids, they can be an alternative solution when very compact devices are needed.

Anticipation

In the foregoing study it was shown that under long-period rapid pulses, viscous dissipation when combined with controllable friction-type dissipation can reduce substantially structural displacements demands by keeping accelerations (base shear) at low levels. Electrorheological dampers or other controllable fluid dampers can produce this type of response. In order to take advantage of the unique rigid-viscoplastic behaviour of ER-dampers, a simple mechanism that will announce the arrival of the strong seismic pulse is needed. A sensor placed in the vicinity of the structure may provide the necessary information about the approaching seismic wave. Although, the electric field in the ER-damper can be activated in

milliseconds, further research is needed to establish practical control strategies to adjust appropriately the electric field.[10]

CONCLUSIONS

In this paper the problem of protecting base-isolated structures from rapid, long-period motions has been addressed. Recent records from near-source earthquakes have created concerns about the vulnerability of flexible structural systems such as base-isolated structures. First, it was shown through a comprehensive analytical study that the presence of friction-type forces (rigid-plastic behaviour) reduces substantially displacements by keeping accelerations (base shears) at low levels. It was found, however, that in some cases the presence of high friction forces in the isolation system of a structure are responsible for the presence of permanent displacements. Electrorheological dampers can, in principle, supply the friction-type forces needed at the beginning of the shaking through their capability of developing rigid-viscoplastic behaviour, but also can eliminate the presence of permanent displacements since the friction forces can be removed at some point during shaking allowing the superstructure to recentre. Finally, it was shown that with the current available technology of electrorheological fluids that ER-dampers, when properly designed, can deliver the level of friction-type forces needed even for large values of design velocities such as 1 m/sec or more. ER-dampers are unique dissipative devices which can effectively protect flexible structures from near-source earthquakes. The construction and testing of the new ER-dampers suitable to enhance the behaviour of base-isolated structures is expected to be completed soon.

ACKNOWLEDGEMENTS

This work is supported by the National Science Foundation Grants BCS-9300827 and CMS-9696241, Dr. S. C. Liu, Program Director. The main cylinder of the damper was manufactured and donated by Taylor Devices, Inc., N. Tonawanda, NY. The constructive comments and suggestions offered by Professor Apostolos Papageorgiou, and Mr. Douglas Taylor are appreciated.

REFERENCES

1. ATC-17-1, *Proc. seminar on seismic isolation, passive energy dissipation, and active control*, Vols. 1 & 2, Applied Technology Council, 1993.
2. M. Campillo, J. C. Gariel, K. Aki and F. J. Sanchez-Sesma, 'Destructve strong ground motions in Mexico City: source, path, and site effects during great 1985 Michoagan earthquake', *Bull. seismol. soc. Am. Vol.* **79**, 1718–1735 (1989).
3. W. D. Iwan and X. D. Chen, 'Important near-field ground motion data from the Landers earthquake', *Proc. 10th European conf. earthquake engrg*, Vienna, 1994.
4. J. F. Hall, 'A ground motion challenge for structural control strategies', *Newslett. IASC* **1**, 2–5 (1995).
5. J. F. Hall, T. H. Heaton, M. W. Halling and D. J. Wald, 'Near-source ground motions and its effects on flexible buildings', *Earthquake spectra* **11**, 569–605 (1995).
6. T. H. Heaton, J. F. Hall, D. J. Wald and M. V. Halling, 'Response of high-rise and base-isolated buildings to a hypothetical Mw 7·0 blind thrust earthquake', *Science* **267**, 206–211 (1995).
7. L. S. Jacobsen and R. S. Ayre, *Engineering Vibrations*, McGraw-Hill, New York, NY 1958.
8. N. Makris and H. Deoskar, 'Prediction of observed response of a base isolated structure', *J. struct. eng.* **122**, 485–493 (1996).
9. N. Makris and M. C. Constantinou, 'Spring–viscous damper systems for combined seismic and vibration isolation', *Earthquake eng. struct. dyn.* **21**, 649–664 (1992).
10. X. Koutsoukos, N. Makris and P. J. Antsaklis, 'Controlling the response of structures equipped with controllable fluid dampers', *Proc. American control conf.* Albourquerque, NM, 1997 (submitted).
11. *Uniform Building Code*, International Conference of Building Officials, Whittier, CA, 1994.
12. N. Makris and M. C. Constantinou, 'Analysis of motion resisted by friction: I. Constant-Coulomb and linear-Coulomb friction', *Mech. struct. mach.* **19**, 477–500 (1991).
13. M. Q. Feng, M. Shinozuka and S. Fujii, 'Friction-controllable sliding isolation system', *J. eng. mech. ASCE* **119**, 1845–1864 (1993).
14. J. N. Yang, J. C. Wu, A. M. Reinhorn and M. Riley, 'Control of sliding-isolated buildings using sliding-mode control', *J. struct. eng. ASCE* **122**, 179–186 (1996).
15. J. D. Carlson and K. D. Weiss, 'A growing attraction to magnetic fluids', *Machine des.* **8**, 61–64 (1994).
16. ENR, 'Hospital girds for quake', *Eng. news record* **11**, 24–26 (1995).
17. N. G. Stevens, J. L. Sproston and R. Stanway, 'Experimental evaluation of a simple electroviscous damper', *J. Electrostatic.* **15**, 275–283 (1984).

18. T. G. Douclos, 'Design of devices using electrorheological fluids', *Soc. automotive eng., Paper* 881134, 2.532–2.536 (1989).
19. R. C. Ehrgott and S. F. Masri, 'Modeling the oscillatory dynamic behaviour of electrorheological materials in shear', *Smart mater. struct.* **1**, 275–285 (1992).
20. H. P. Gavin and R. D. Hanson, 'Electrorheological dampers for structural vibration suppression', *Report No. UMCEE 94-35*, Dept. Civil and Envir. Engrg, University of Michigan, Ann Arbor, MI 1994.
21. N. Makris, S. A. Burton, D. Hill and M. Jordan, 'Analysis and design of an electrorheological damper for seismic protection of structures', *J. eng. mech. ASCE* **122**, 1003–1011 (1996).
22. R. W. Phillips, 'Engineering applications of fluids with variable yield stress', *Ph.D. Dissertation*, University of California, Berkeley, CA, 1969.
23. A. Pinkos, E. Shtarkman and T. Fitzgerald, 'Active damping using ERM fluids', *Automotive Eng.* **6**, 19–23 (1993).
24. H. Schlichting, *Boundary-Layer Theory*, McGraw-Hill, New York, NY, 1987.

